Journal of Power Sources 189 (2009) 730–732

Contents lists available at ScienceDirect

Journal of Power Sources

journal homepage: www.elsevier.com/locate/jpowsour

Short communication

Preparation and electrochemical performance of Sn–Co–C composite as anode material for Li-ion batteries

Zhongxue Chen, Jiangfeng Qian, Xinping Ai, Yuliang Cao*, Hanxi Yang

Department of Chemistry, Hubei Key Laboratory of Electrochemical Power Sources, Wuhan University, Wuhan 430072, China

ARTICLE INFO

Article history:
Received 20 June 2008
Received in revised form 13 August 2008
Accepted 14 August 2008
Available online 22 August 2008

Keywords:
Sn–Co–C
Alloy
Polymer-pyrolysis method
Lithium-ion battery

ABSTRACT

A Sn–Co–C composite was prepared by a polymer-pyrolysis route followed with ball milling. The structural and morphological features of the Sn–Co–C composite were characterized by powder X-ray diffraction and scanning electron microscope. The experimental results revealed that the Sn–Co–C composite can deliver a high reversible capacity of 486 mAh g^{-1} after 40th cycle. This suggests that the polymer-pyrolysis method provides a possible alternative for preparation of the alloy anode for lithium-ion batteries.

1. Introduction

Lithium–tin alloys have been focused as an attractive alternate material of conventional graphite for advanced lithium-ion batteries due to its very high lithium storage (994 mAh g^{-1} for $Li_{4.4}Sn$), large packing density and safe thermodynamic potential [1]. However, the most critical problem preventing from the commercial application of the lithium–tin alloys is its severe volumetric changes during charge and discharge [2], which result in cracking and pulverization of the material, leading to a rapid capacity fading. Accordingly, great efforts have been devoted to overcome this problem in order to use the appealing materials in commercialized lithium batteries. A promising approach is to use intermetallic compounds or active/inactive composites, for example Sn–Co [3], Sn–Co–C [4], Sn–Cu [5], Sn–Ni [6], etc. These materials exhibit improved cycling performance due to the buffering effect of inactive components in the alloys, which provide structural stability during cycling [7]. Sn–Co–C composites have recently attracted great attentions since Sony Company used this new material for commercial battery applications [8].

In previous studies, there have been a number of reports for preparation and electrochemical properties of Sn–Co composites [9–12]. Dahn et al. prepared the ternary Sn–Co–C libraries extending over hundred different compositions by using combinatorial and high-throughput analysis method and pointed out that the amorphous nano-structured Sn–Co–C alloys exist only in a very narrow composition range and may exhibit good cycling stability [12]. Hassoun et al. synthesized a ternary $Sn_{0.31}Co_{0.28}C_{0.41}$ composite by high energy ball milling and revealed that longer milling time led to the formation of a single homogeneous phase and the amorphous structure of Sn–Co–C favors to improve the cycling performance of the alloy anode [9].

In this work, we prepared the ternary Sn–Co–C composites by a polymer-pyrolysis method [13] and investigated the structural and electrochemical properties of the as-prepared composites as an anode material for lithium-ion batteries.

2. Experimental

The Sn–Co–C composites were prepared by pyrolysis of the copolymeric acrylate precursor of Sn and Co. The polymeric precursor was synthesized by dissolving stoichiometric SnO_2 and $Co(NO_3)_2{\cdot}6H_2O$ in acrylic acid (Sn:Co:AA = 2:1:15 in molar ratio) and copolymerizing the acrylates by adding a small amount of $(NH_4)_2S_2O_8$ initiator in the solution at continuous stirring at 80 °C. The polymeric precursor as formed was dried at ~100 °C and then pyrolyzed in an inert (pure argon) atmosphere at 900 °C for 3 h. When cooled to the room temperature, the obtained sample was milled in a planetary miller (QM-1SP04, Nanjing, China) for 48 h with the weigh ratio of powder to balls of 1:20. The milling pot contains 1 g active material, three 3.3 g balls and fourteen 0.75 g balls using a rotation speed of 240 rpm. To prevent metal oxi-

* Corresponding author. Tel.: +86 27 68754526; fax: +86 27 87884476.
E-mail address: ylcao@whu.edu.cn (Y. Cao).

0378-7753/$ – see front matter © 2008 Elsevier B.V. All rights reserved.
doi:10.1016/j.jpowsour.2008.08.027

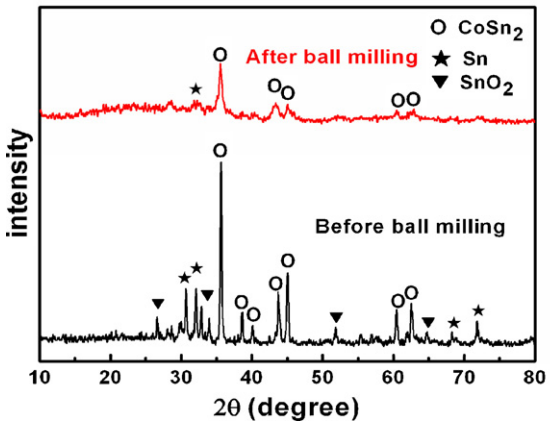

Fig. 1. XRD patterns of the Sn–Co–C composite before and after ball milling.

dation during milling, powder handling was performed under a purified Ar atmosphere. The actual stoichiometric amount of Sn and Co of the as-prepared Sn–Co–C composite was determined by inductively coupled plasma (ICP) analysis. The amount of carbon in the as-prepared Sn–Co–C composite was weighed after dissolving the composite by the mixture of HCl and HNO_3. The result shows that the composition of the final product is expressed as $Sn_{64.0}Co_{15.6}C_{15.5}O_{4.9}$ (wt.%).

The structural and surface morphology of the as-prepared Sn–Co–C composite were characterized by X-ray diffraction (XRD, Shimadzu XRD-6000) using Cu Kα radiation and scanning electron microscopy (SEM, Quanta200, FEI, Netherlands).

The Sn–Co–C anode for electrochemical measurements was prepared by mixing 80 wt.% active material, 12 wt.% acetylene black and 8 wt.% PTFE into paste, then rolling the pasted mixture into ca. ~0.1 mm thick electrode sheet, and finally pressing the electrode sheet onto a nickel foam. The charge–discharge experiments were carried out on the test cells of a three-electrode design with reference to Li counter electrode. The separator was Celgard 2400 microporous membrane. The electrolyte was 1 M $LiPF_6$ dissolved in a mixture of ethylene carbonate (EC), dimethyl carbonate (DMC) and ethylene methyl carbonate (EMC) (1:1:1 by wt., Shinestar Battery Materials Co., Ltd., China). The area of test electrode is about 1.5 cm^2. The test cells were assembled in an argon-filled glove box and galvanostatically charged and discharged over a voltage range of 0.02–1.5 V at a current density of 100 mA g^{-1} (~0.5 mA cm^{-2}) by battery tester (BTS-55 Neware Battery Testing System, Shenzhen, China). The electrochemical tests were carried out at room temperature.

3. Results and discussion

Fig. 1 displays the XRD patterns of the Sn–Co–C composite before and after ball milling. Before planetary ball milling, the samples showed a number of XRD peaks, in which the peaks at 35.5°, 38.6°, 40.0°, 43.6°, 45.0°, 60.3° and 62.4° can be all indexed by tetragonal $CoSn_2$ (JCPDS No. 65-2697, space group: *I*4/*mcm*, 140) and the main double peaks at 30.6° and 32.0° can be attributed to tetragonal Sn (JCPDS No. 89-4898, space group: *I*4/*amd*, 141). The appearance of few weak XRD signals of SnO_2 phase suggests that there still existed small amount of SnO_2 phase in the samples. The XRD data indicated that tin and cobalt oxides were mostly reduced to form $CoSn_2$ and Sn. After ball milling, the main peaks of Sn and $CoSn_2$ could still be clearly observed but became weaker and broader, implying a decrease in the particle size or in the crystallity of the alloy compound. Therefore, it is expected that such a change could provide the as-prepared composite to accommodate a large volumetric and structural change during cycling.

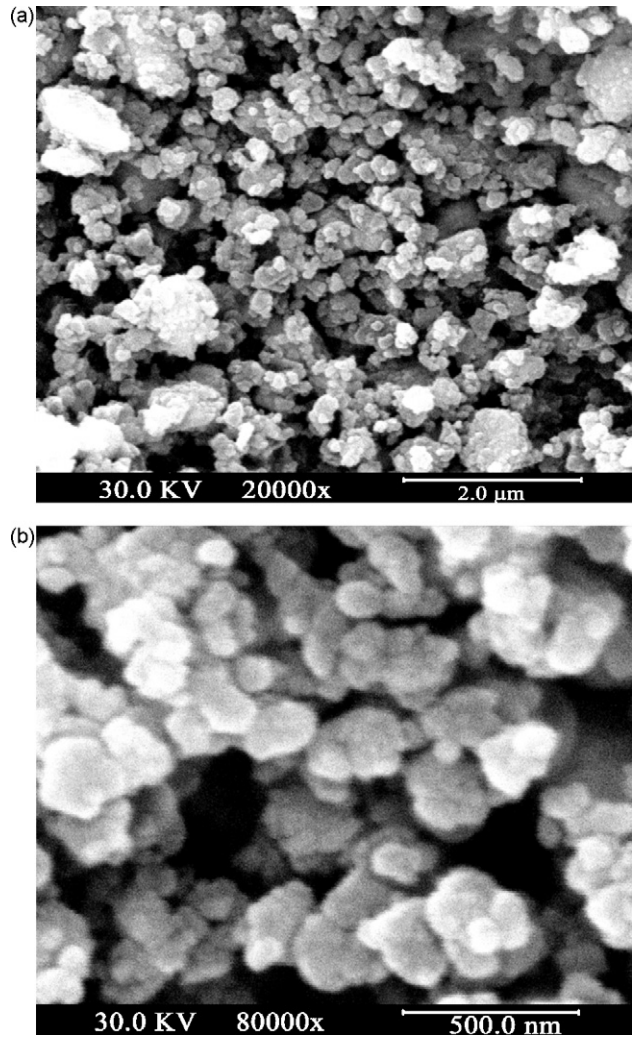

Fig. 2. SEM image (a) and amplified image (b) of the Sn–Co–C composite after ball milling.

Fig. 2 shows the SEM images of the Sn–Co–C composites after ball milling. As it can be seen in Fig. 2, the Sn–Co–C alloy powders are composed of small particles with an average size of ca.100 nm. This morphological feature of the Sn–Co–C composite suggests that the polymer-pyrolysis method would be favor to produce the uniformly distributed precursor.

Fig. 3 shows the charge and discharge curves of the Sn–Co–C composite electrode at constant current of 100 mA g^{-1}. In first cycle, the Sn–Co–C electrode showed a large charge (lithium alloying) capacity of 1137 mAh g^{-1} while the corresponding discharge (lithium dealloying) capacity is 451 mAh g^{-1} apparently due to a huge irreversible reaction taking place at the potential range of 1.5–0.75 V (vs. Li/Li^+). This irreversible capacity arises most likely from the following reasons: (1) the formation of SEI film on the surface of the metal Sn and pyrolytic carbon [14], (2) the reduction of residual SnO_2, (3) the presence of abundant unsaturated carbon atoms on the pyrolytic samples, which may catalyze the decomposition of electrolytes. However, since the second cycle, the alloy anode delivered a discharge capacity very close to its charging capacity with coulomb efficiency of ≥90%, after 5 cycles, the coulombic efficiency shifted to 95% and became stable afterwards, suggesting a good electrochemical reversibility of this material.

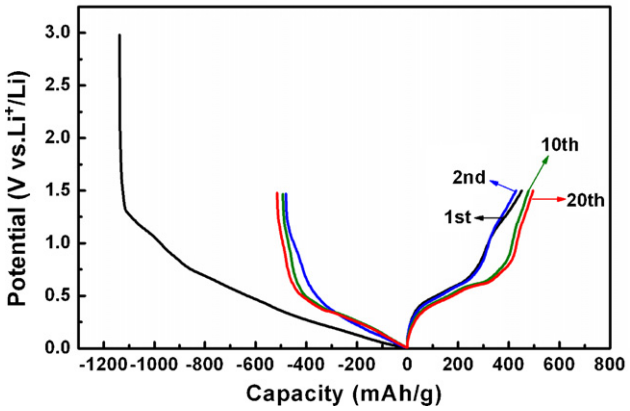

Fig. 3. Charge/discharge curves of the Sn–Co–C composite.

Fig. 4 gives the cycling performance of the Sn–Co–C composite electrode. The reversible capacity of the Sn–Co–C electrode varied from initial 451 mAh g^{-1} to slightly higher value of 486 mAh g^{-1} in the 40th cycle, showing excellent cycleability of the alloy material. This cycling stability can be attributed to the stable matrix formed by inactive component Co and pyrolytic carbon, which effectively restrains cracking and pulverization of tin particles. However, a major drawback of this material is its relatively low initial coulombic efficiency (~40%) due to the presence of unreacted SnO_2 and large active surface of carbon. In despite of this, the coulombic efficiency rose to 94% in three cycles, suggesting that once the stable SEI layer is formed, the composite anode should display quite high charge–discharge efficiency [15].

To observe the structural change of the Sn–Co–C composite during charge and discharge, we carried out the XRD measurements of the alloy anode at different cycles. As shown in Fig. 5b, after 1st charge, the 31° diffraction peaks of Sn-phase became almost invisible and correspondingly a board peak characteristic of Li_xSn alloy emerged at 23°, suggesting the formation of Li_xSn phase upon lithium insertion. In comparison with previously reported data [16], the XRD peak of Li_xSn alloy is much weaker and broader, implying that Li_xSn alloy formed during charge has a lower crystallity or a smaller size in our experiment. At the same time, the main XRD peak of $CoSn_2$ at 35° was still observable but became weaker and broader after first charge. This phenomenon suggests that the $CoSn_2$ phase did not play a dominative contribution for lithium insertion but contributed only a small part for the formation of Li_xSn alloy. After 1st discharge (Fig. 5c) the XRD signals of Li_xSn phase vanished while the XRD peaks characteristic of elemental Sn

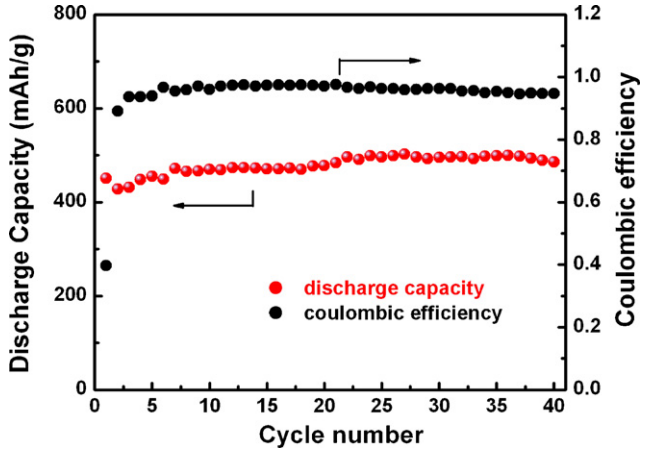

Fig. 4. Reversible capacities and coulombic efficiency of the Sn–Co–C composite.

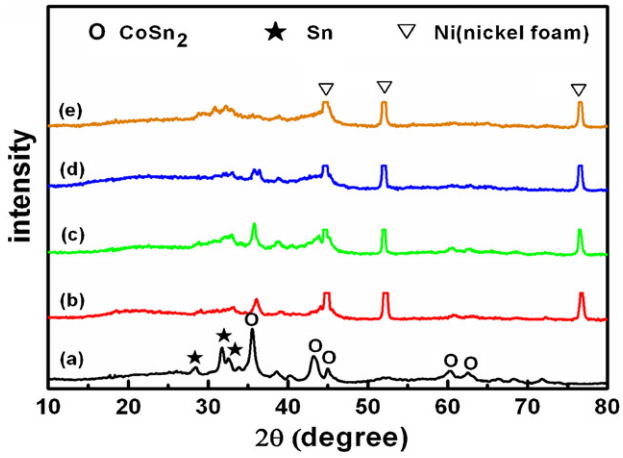

Fig. 5. XRD patterns of the Sn–Co–C electrode: (a) before cycling test; (b) after 1st discharge; (c) after 1st charge; (d) after 3rd charge; (e) after 40th charge.

reappeared, further convincing that the metallic Sn dispersed in the $CoSn_2$ matrix is the main active centers for alloying and dealloying reaction of lithium. In subsequent cycling, the XRD signal of $CoSn_2$ phase gradually decreased and disappeared after 40th cycle (see Fig. 5e), indicating the alloying reaction of $CoSn_2$ with lithium took place to form Li_xSn and amorphous Co [16]. This explanation may be taken into account for the gradually increased capacity observed for the as-prepared Sn–Co–C composite with cycling.

4. Conclusions

This paper describes the structural and electrochemical property of Sn–Co–C composition prepared by a polymer-pyrolysis route followed with ball milling. The experimental results exhibit that the Sn–Co–C composite is composed of uniformly distributed, nano-sized particles and can deliver a high initial capacity of 451 mAh g^{-1} and remain a reversible capacity of 486 mAh g^{-1} after 40th cycle, performing excellent capacity retention.

Acknowledgements

We acknowledge financial support by the 973 Program, China (Grant 2009CB220100) and the National Science Foundation of China (No. 50502025).

References

[1] J.M. Tarascon, M. Armand, Nature 414 (15) (2001) 359–367.
[2] R. Benedek, M.M. Thackeray, J. Power Sources 110 (2002) 406–411.
[3] N. Tamura, M. Fujimoto, M. Kamino, S. Fujitani, Electrochim. Acta 49 (2004) 1949–1956.
[4] J. Hassoun, S. Panero, G. Mulas, B. Scrosati, J. Power Sources 171 (2007) 928–931.
[5] J. Wolfenstine, S. Campos, D. Foster, J. Read, W.K. Behl, J. Power Sources 109 (2002) 230–233.
[6] J. Hassoun, S. Panero, P. Simon, P.L. Taberna, B. Scrosati, Adv. Mater. 19 (2007) 1632–1635.
[7] M. Winter, J.O. Besenhard, M.E. Spahr, P. Novak, Adv. Mater. 10 (1998) 725.
[8] S. Kawakami, M. Asao, US Patent 6,949,312 (2005).
[9] J. Hassoun, G. Mulas, S. Panero, B. Scrosati, Electrochem. Commun. 9 (2007) 2075–2081.
[10] M.S. Park, S.A. Needham, G.X. Wang, Y.M. Kang, J.S. Park, S.X. Dou, H.K. Liu, Chem. Mater. 19 (2007) 2406–2410.
[11] H. Guo, H.L. Zhao, X.D. Jia, Electrochim. Acta 52 (14) (2007) 4853–4857.
[12] J.R. Dahn, R.E. Mar, Alyaa Abouzeid, J. Electrochem. Soc. 153 (2) (2006) A361–A365.
[13] L.H. Yu, H.X. Yang, X.P. Ai, Y.L. Cao, J. Phys. Chem. B 109 (2005) 1148–1154.
[14] M.R. Wagner, P.R. Raimann, A. Trifonova, K.-C. Moeller, J.O. Besenhard, M. Winter, J. Electrochem. Soc. 7 (7) (2004) A201–A205.
[15] T. Li, Y.L. Cao, X.P. Ai, H.X. Yang, J. Power Sources (2008).
[16] J.J. Zhang, Y.Y. Xia, J. Electrochem. Soc. 153 (8) (2006) A1466–A1471.